PHILOSOPHICAL TRANSACTIONS OF THE ROYAL SOCIETY A MATHEMATICAL, PHYSICAL & ENGINEERING SCIENCES

Heterostructure Barrier Varactors at Submillimetre Waves

Erik L. Kollberg, Jan Stake and Lars Dillner

Phil. Trans. R. Soc. Lond. A 1996 **354**, 2383-2398
doi: 10.1098/rsta.1996.0106

Heterostructure barrier varactors at submillimetre waves

By Erik L. Kollberg, Jan Stake and Lars Dillner

The Millimetre Wave Group, Department of Microwave Technology, Chalmers University of Technology, 412 96 Göteborg, Sweden

We present an overview of recent results concerning quantum barrier varactors, also called heterostructure barrier varactors (HBV). This device is normally constructed as a mesa device, with one or several thin (*ca.* 200 Å) barriers made from a larger bandgap material. The diodes are excellent as multipliers and have several advantages over the common Schottky barrier varactor. The HBV only generates odd harmonics of the input power, can be built to handle large powers and permits a large device area at very high frequencies. We present theoretical design and performance characteristics for triplers and quintuplers and give an overview of HBV multiplier experiments.

1. Introduction

Varactor multipliers are frequently used to generate power at radio frequencies up to submillimetre-wave frequencies. The varactor multiplier uses a nonlinear capacitance to transform power at a frequency f_p to power at $n\,f_p$. Competing methods are based on direct power generation, e.g. using negative resistance devices such as Gunn or IMPATT diodes, or transistors for transforming DC power to RF power (for a survey see Yngvesson 1991). A general problem while going to higher frequencies is that the output power becomes smaller. The main reason for this is that shorter distances (device dimensions) are necessary for the electrons to do a faster job. The shrinking dimensions (volume) and the decreasing DC to RF power efficiency (typically 5% at around 100 GHz) creates a heating problem. For better power handling we need a device that has large dimensions and high efficiency.

The most common type of varactor, the Schottky diode, suffers from the limitations mentioned above. The heterostructure barrier varactor (HBV), however, has the potential to avoid several of these problems. HBV diodes have so far been realized in a mesa-type structure, where a barrier consisting of a thin layer of high bandgap material prevents conduction electrons from passing and causes a depleted region to build up when the diode is biased (see the following). The diode was first called the quantum barrier varactor (QBV), later the 'single-barrier varactor' (SBV), and now the 'heterostructure barrier varactor' (HBV).

The particular advantage of the HBV is its symmetric capacitance–voltage (CV) characteristic, which ensures that only odd harmonics are generated (see below). Competing symmetrical devices are the back-to-back barrier–N–N^+ (bbBNN$^+$) (Lieneweg *et al.* 1987) diode, which is essentially a planar diode with two Schottkys back to back and the Schottky/2DEG/Schottky diode (Peatman *et al.* 1992).

Phil. Trans. R. Soc. Lond. A (1996) **354**, 2383–2398
Printed in Great Britain

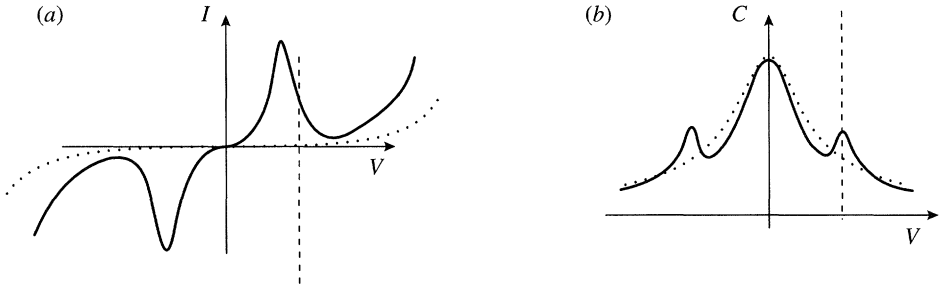

Figure 1. The current–voltage (I–V) and capacitance–voltage (C–V) characteristic of a double-barrier resonant tunnelling diode. The dashed curve indicates the I–V and C–V characteristics for thick barriers.

2. Background

The idea of the HBV diode came about during work on the double-barrier resonant tunnelling diode, which is a promising candidate for generating power at millimetre and submillimetre waves. The current–voltage (IV) characteristic shows a negative resistance region (figure 1), which can be utilized in negative resistance oscillators (Sollner *et al.* 1987). Since the capacitance is much lower than for the traditional tunnel diode, the efficiency will remain substantial to quite high frequencies.

It has also been realized that the resonant tunnelling diode, due to its strongly nonlinear impedance characteristic, has a potential use in multipliers for millimetre-wave power generation (Rydberg & Grönqvist 1989). It is not only the IV characteristic (figure 1*a*) which is strongly nonlinear, but also the capacitance–voltage characteristic (see figure 1*b*).

It seems obvious that the diode should be efficient when used in a multiplier. Hence by driving the diode with a sinusoidal voltage at frequency f_p, the resulting current through the diode will contain harmonic components at $n\,f_\mathrm{p}$, i.e. power will be generated at these harmonic frequencies. This idea has been tried successfully (Rydberg & Grönqvist 1989); however, a careful analysis of the detailed process showed that it was not so much the nonlinearity in the IV characteristic, which contributed most to the efficiency, it was the nonlinear CV characteristic. There is a peak in the CV, which is of little importance for the multiplier efficiency, essentially because the pump voltage will drive the IV far beyond the peak. This peak occurs at the bias voltage of maximum negative conductance and is caused by the change in charge stored in the diode related to the conduction current. In the graph is also shown the expected CV if no conduction current was present (dashed curve).

These facts made it obvious to try a multiplier diode without a resonant tunnelling double-barrier structure and only use one single barrier to prevent majority carriers from moving from anode to cathode and allow voltage-dependent depletion regions to develop. The quantum barrier varactor or as it was later called the heterostructure barrier varactor was born (Kollberg & Rydberg 1989).

3. The multiplier

Of basic importance is the *efficiency* of a multiplier, i.e. the ratio of the output power to the input power:

$$\text{efficiency} = \frac{P_\mathrm{out}(nf_\mathrm{p})}{P_\mathrm{int}(f_\mathrm{p})}. \tag{3.1}$$

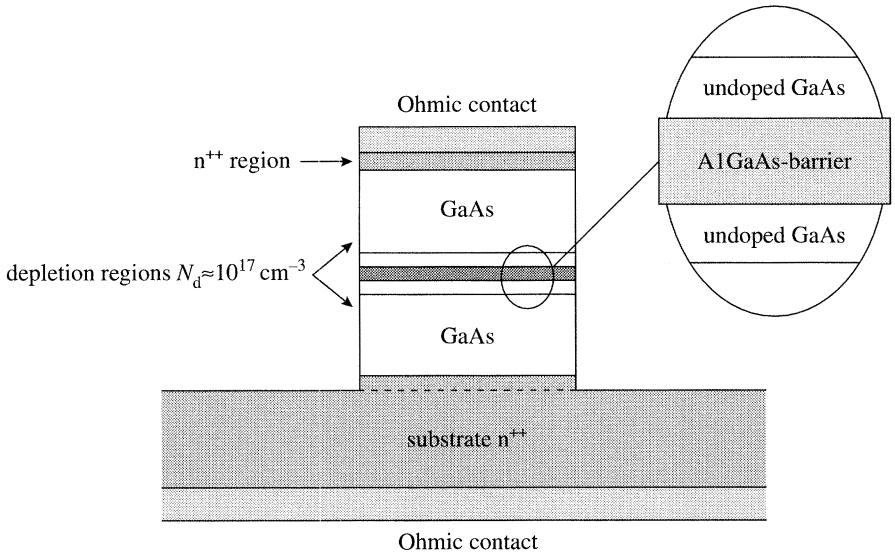

Figure 2. Schematic description of a HBV with one barrier. This particular type of diode design can be soldered and bonded (on the top contact) into a multiplier circuit.

If the input is matched, i.e. no power is reflected, the input pump power will emerge in two ways. One part will emerge as power at harmonic frequencies and another part will be absorbed in resistive parts of the diode (modelled as a series resistance). The multiplier circuit must be designed so that maximum power emerges at the *required harmonic frequency*.

It is important that the *impedance properties* of the pumped diode are such that it is reasonably easy to arrange for (near) optimum embedding impedances, at least at the input and the output frequency. It is not usually so important to consider impedances at higher harmonics than the output frequency.

Another important characteristic is the *power handling capability*. The HBV diode has some particular advantages in this respect: it is possible to build material yielding a stack of series coupled diodes (see § 4 *b*).

4. Basic diode design considerations

In figure 2, the design of a basic HBV diode is described. The device, has a thin layer (a few hundred Å) of a large bandgap material that acts as a barrier and a thicker layer (typically a few thousand Å) of a smaller bandgap material allowing depletion regions to develop on each side of the barrier (Kollberg & Rydberg 1989; Rydberg *et al.* 1990, 1992; Grönqvist *et al.* 1991; Tolmunen *et al.* 1991; Kollberg *et al.* 1992). At both sides of the barrier a thin layer of undoped low bandgap material is usually included. Further details will be described below in § 4 *c*.

In figure 3 we describe the conduction band potential for a certain bias voltage V_{bias}, As shown in figure 4, the capacitance, proportional to $1/W$, is obviously symmetrical around zero bias, and the IV is anti-symmetrical.

The equivalent circuit of this diode is shown in figure 4. An important feature of the capacitance characteristic is the ratio between $C_{\max}$ and $C_{\min}$. If there is no difference there cannot be any harmonic generation. This question will be discussed further in § 5.

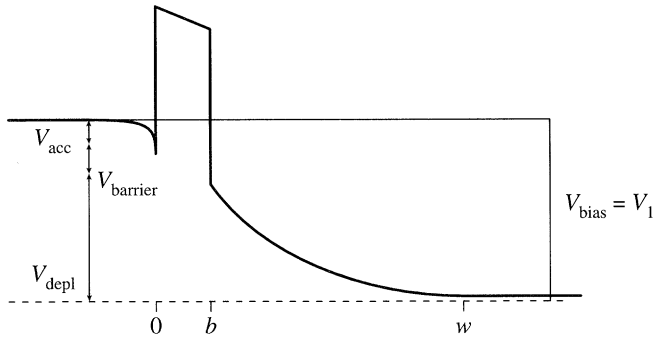

Figure 3. The conduction band potential for a bias voltage $V_{bias} = V_{acc} + V_{barrier} + V_{depl}$.

Since the capacitance is an even function of the applied voltage and the capacitive current is $C(V(t))(\mathrm{d}V(t)/\mathrm{d}t)$ and since the conduction current is an odd function of the applied voltage, i.e. proportional to $V(t)R_p(V(t))$ where $R_p(V(t))$ is also an even function of $V(t)$, a sinusoidal pump voltage will create only odd harmonic current components. This means that there are no circuit considerations at even harmonics. This is contrary to the Schottky diode tripler where there is one important idler frequency termination at the second harmonic that must be optimized in order to maximize the efficiency. For the Schottky diode quintupler ($\times 5$) one has to optimize terminations at three idler frequencies ($\times 2$, $\times 3$ and $\times 4$). Since a multiplier using a HBV does not generate any even harmonics an optimized tripler or a quintupler will be considerably easier to realize in practice. Losses will as well be smaller, since no power can be lost at any even harmonic. The circuit design and the mechanical construction of a higher order multiplier using a HBV device is consequently much easier compared to one which uses a Schottky diode. Another complication in designing the circuit of a Schottky diode multiplier is that the diode usually needs a DC bias voltage for optimum operation, while the HBV multiplier is operated with zero bias voltage.

The parallel resistance $R_p(V(t))$ can be determined from the IV characteristic. The DC current through a good diode is basically determined by thermionic emission of electrons over the barrier and can be kept small if the barrier is high and broad. When $\mathrm{d}V/\mathrm{d}I$ derived from $V = V_{max}$ is much larger than $1/(2\pi f_p C_{min})$, R_p in figure 4 can be neglected. Actually, analysis shows (Nilsen *et al.* 1993; Krishnamurthi *et al.* 1994*b*) that the IV or (R_p) always influences the efficiency in a negative way. In general $\mathrm{d}V/\mathrm{d}I \gg 1/(2\pi f_p C_{min})$, i.e. R_p in figure 3, can indeed be neglected.

The series resistance is due to ohmic losses in the bulk of the semiconductor, both in the mesa and in the substrate and in the ohmic contact. R_s, of course, should be as small as possible. It is convenient to define a 'cut-off' frequency f_c, namely

$$f_c = \frac{1}{2\pi R_s}\left(\frac{1}{C_{min}} - \frac{1}{C_{max}}\right). \tag{4.1}$$

A more accurate theoretical model has been presented (Jones *et al.* 1994, 1995) utilizing a hydrodynamic device simulation method integrated with a harmonic balance circuit analysis technique. A particular problem is related to the fact that electrons in semiconductors cannot move with a speed higher than a certain limiting speed v_{max}. This means that for a certain charge density 'n' in the semiconductor, there is a certain maximum current density $j_{max} = nev_{max}$, where e is the charge of the electron. Consider an ideal varactor $C(v)$, in series with a resistance R_s.

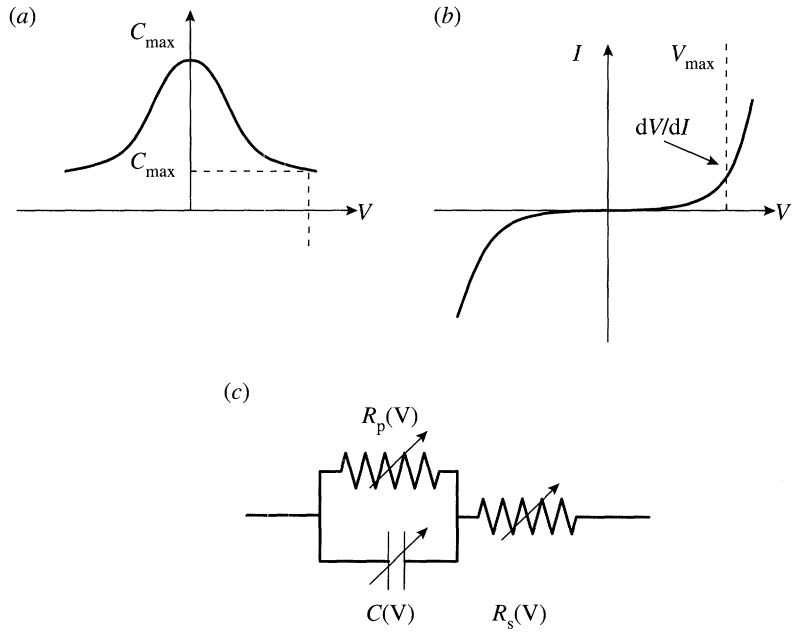

Figure 4. (*a*) a typical capacitance versus voltage characteristic, (*b*) a typical current–voltage characteristic and (*c*) the equivalent circuit for the HBV.

The displacement current i_d must equal the electron conduction current, i_e (compare with figure 5). We get

$$C_d \frac{dV(t)}{dt} = A_d n_e v_e(t) e, \tag{4.2}$$

where $C_d(t)$ is the depletion capacitance and $V_d(t)$ is the voltage over the depletion region. A_d is the diode area, n_e the electron density (in our case $n_e \approx N_d$, the doping density), v_e the electron velocity and e the charge of the electron. Hence we expect the capacitive current $i_d(t)$ to increase with the pump power and the pump frequency. The electron velocity v_e in semiconductors cannot go above v_{max} (for GaAs v_{max} is about 2×10^5 m s^{-1} at about 3.2 kV cm^{-1} (Sze 1981)). Hence, there will occur a saturation phenomenon in the current when $i_d \to i_{sat}$, where

$$i_{sat} = A_d n_e v_{max} e. \tag{4.3}$$

This current-limiting phenomenon can be modelled as an effective series resistance (Kollberg *et al.* 1992), which increases rapidly with higher power (or equivalently high current), causing considerable deterioration in the multiplier performance. Allowing a two- to threefold increase in the series resistance for $i = i_{sat}$, this model describes quite well the situation in Schottky varactor multipliers. The same phenomenon will, of course, take place also in HBV multipliers.

The influence of the current saturation at, for example, several hundred GHz or a THz, will become quite severe. Calculations involving Monte Carlo simulations (Kollberg *et al.* 1992) indicate that the efficiency of a Schottky tripler with an output frequency of 1 THz may only be 5% of the efficiency obtainable if there were no current saturation phenomenon.

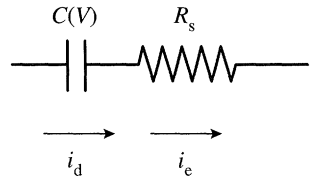

Figure 5. Device equivalent circuit used for the analysing current saturation.

5. Stacked diodes

As was already mentioned, it is possible to fabricate epitaxial material that will allow design of a stacked diode varactor (figure 6). This arrangement has several advantages.

(*a*) *Power handling*

Let us assume that a diode has n barriers and $n+1$ depletion regions. Each 'diode' can be biased with a voltage as indicated in equation (5.1) and figure 3. Hence the total voltage becomes

$$V_{\text{total}} = nV_1, \tag{5.1}$$

where V_1 is the voltage for a diode with one barrier only. If we have n stacked diodes, we must also scale the area with n in order to have the impedance $Z = V_{\text{total}}/I_{\text{total}}$ the same as for one barrier diode. Hence, the power the diode can now handle is $V_{\text{total}}I_{\text{total}} = n^2V_1I_1$ or n^2 as large as for a one barrier diode. Also notice that the increased area of the diode improves the cooling of the diode, which may be quite important in allowing high power handling.

(*b*) *Series resistance*

For an area n times larger, an n times lower ohmic contact is obtained. The mesa resistance remains the same, while the substrate (spreading) resistance also becomes smaller. This effect will, of course, increase the efficiency considerably.

(*c*) *Current saturation*

Another effect of using the stacked diode design is that the problems related to the current saturation phenomenon are much less severe. First consider a Schottky diode varactor with the same large area as, for example, a 10-barrier diode. In order to allow the same minimum capacitance, the maximum depletion region width ($W_{\max}$) must be the same. Hence in the Schottky diode electrons will have to travel over a distance determined by the ratio of $W_{\max}(1-C_{\min}/C_{\max})$ while in the 10-barrier HBV electrons only have to travel only 1/10 of the same distance. Since the electrons should follow the function $\sin(n2\pi ft)$ the problem will show up at high enough frequencies. If the electrons have to travel 2 μm in half a period at say 200 GHz, the maximum speed of the electrons must be more than 10^6 m s^{-1}, well above the maximum speed allowed in known semiconductors (a factor of 5 compared with $v_{\max}$ in GaAs!). For the Schottky diode case a quite (unrealistically) low doping is necessary to allow the depleted region to extend over 2 μm. This will, of course, mean a large series resistance. In the 10-barrier HBV, all these effects are relaxed with a factor of 10.

(*d*) *Contacting*

Due to the larger area of the stacked diode, contacting will become a much smaller problem. This will facilitate using the diode as a whisker-contacted diode

PHILOSOPHICAL TRANSACTIONS OF THE ROYAL SOCIETY A MATHEMATICAL, PHYSICAL & ENGINEERING SCIENCES

in waveguides for submillimetre multipliers, designing high power planar structures at millimetre-wave frequencies and bonding the diode into a circuit for microwave or (low-frequency) millimetre-wave applications. Comparing the stacked diode with, for example, the bbBNN$^+$ diode (Lieneweg *et al.* 1987) there is certainly more flexibility in designing stacked diodes. They can be stacked, and a variety of materials combinations can be used.

6. The shape of the capacitance versus voltage curve

It was mentioned in § 4 that the ratio $C_{\max}/C_{\min}$ is an important parameter. An elegant and analytically powerful method to describe the CV characteristic was introduced by Krishnamurthi & Harrison (1993) and extended by Dillner *et al.* (1995). The voltage over the capacitance is described in terms of a power series of the charge q accumulated in the diode (Tang 1966):

$$V = \alpha q + \beta \frac{q^3}{q_{\max}^2} + \gamma \frac{q^5}{q_{\max}^4}. \tag{6.1}$$

From this equation the capacitance $C(V)$ is obtained as $\mathrm{d}q/\mathrm{d}V$. The parameters of equation (6.1) can be evaluated for different cases in order to investigate how the varactor performance depends on the shape of the $C(V)$ characteristic. We have chosen three special cases, where

$$\alpha = \frac{C_{\max}}{C_{\min}}, \tag{6.2}$$

and for

flat $C(V)$: $\beta = 0$, $\gamma = \frac{1}{5}(1 - C_{\min}/C_{\max})$,

cubic model: $\beta = \frac{1}{3}(1 - C_{\min}/C_{\max})$, $\gamma = 0$ (Krishnamurthi *et al.* 1993),

sharp $C(V)$: $\beta = \frac{2}{3}(1 - C_{\min}/C_{\max})$, $\gamma = -\frac{1}{5}(1 - C_{\min}/C_{\max})$.

In figure 6 I show CV characteristics for the three different cases. CV characteristics for experimental diodes typically correspond to a case between 'Flat $C(V)$' and 'Sharp $C(V)$'.

7. Tripler analysis

For $\gamma = 0$, the tripler can now be analysed using closed-form expressions (Krishnamurthi & Harrison 1993) For $\gamma \neq 0$ we have used the harmonic balance method.

The influence of the ratio $C_{\max}/C_{\min}$ is illustrated in figure 8. The graphs are made for the cubic model, $\gamma = 0$. The efficiency increases rapidly as the ratio increases from 1. For $C_{\max}/C_{\min} \to \infty$, the efficiency for each value of the series resistance reaches a constant value.

If the multiplier input frequency f_{p} is normalized to the cut-off frequency, the maximum efficiency is a function of only this variable, i.e. independent of the value of the ratio $C_{\max}/C_{\min}$. In figure 9, the efficiency versus $f_{\mathrm{p}}/f_{\mathrm{c}}$ is depicted.

8. Quintupler analysis

The quintupler is analysed in a similar way to the tripler. In this case, however, it is important to take into account the embedding impedance at the idler frequency

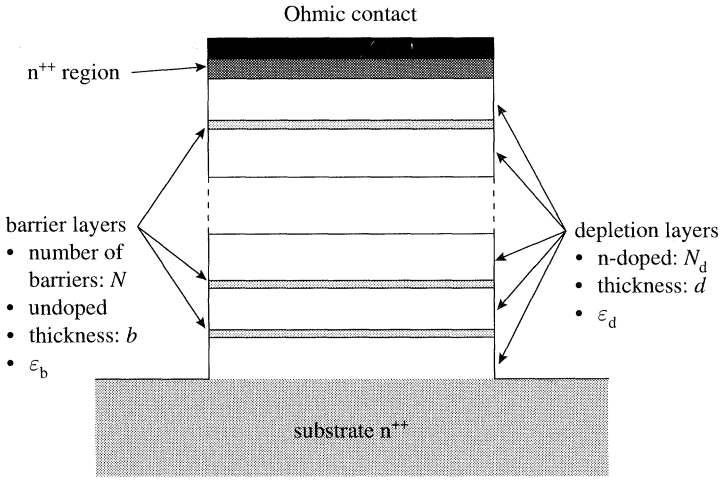

Figure 6. Schematic diagram of a stacked HBV diode. Typically the barrier thickness is 200 Å and the depletion layer thickness 2000 Å.

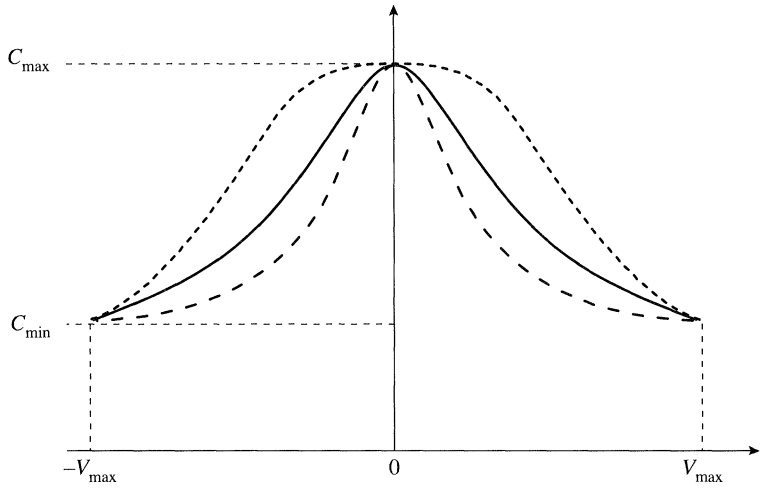

Figure 7. CV characteristic generated from the v–q model, see equation (6.1). ——, Cubic model; - - - -, flat $C(V)$; – – –, sharp $C(V)$.

Z_3 at $3f_p$. We have illustrated this by considering three cases:

case A: $Z_3 = \infty$ (open circuited idler),

case B: $Z_3 = 0$ (short circuited idler),

case C: $Z_3 = \mathrm{j}X_3$ (inductance in resonance with the diode capacitance).

It is an interesting fact that for the cubic model and with the idler open circuited (case A), the diode generates no fifth harmonic current at all, i.e. the quintupler efficiency is zero. If $\gamma \neq 0$ the current at the fifth harmonic will become finite even for case A (see figure 10). The most efficient case is when the idler is loaded with an inductance $\mathrm{j}X_3$ which basically forms a series resonance with the 'mean capacitance' of the diode at the idler frequency. This is illustrated in figure 10.

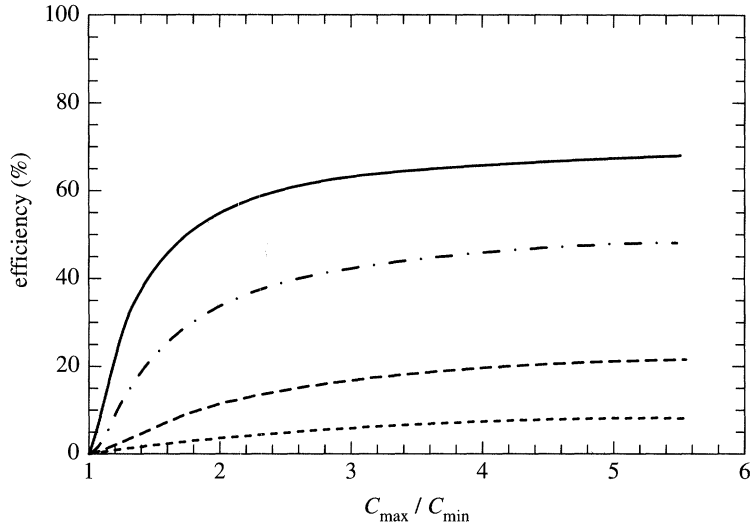

Figure 8. Efficiency versus C_{max}/C_{min} and different values of the series resistance. It is assumed that $1/(2\pi f_p C_{min}) = 100\ \Omega$. ——, $R_s = 1$; – · – · –, $R_s = 2$; – – –, $R_s = 5$; - - - -, $R_s = 10$.

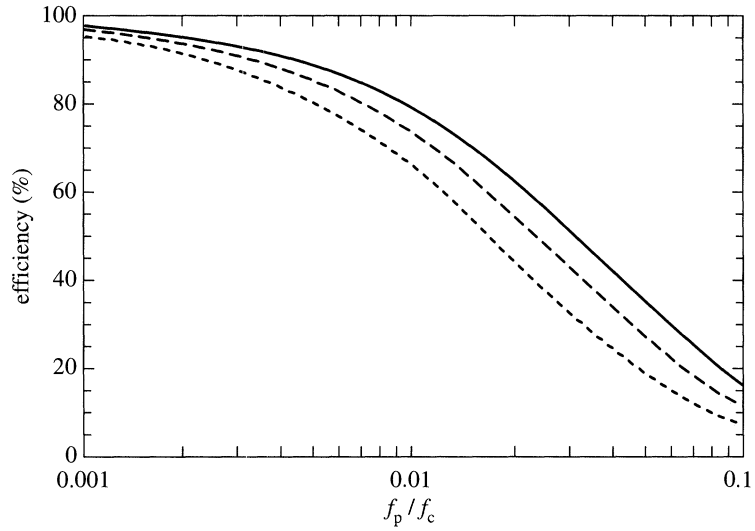

Figure 9. The maximum efficiency for a tripler for different shapes of the CV characteristics. All embedding impedances are adjusted for maximum efficiency. ——, Sharp $C(V)$; – – –, flat $C(V)$; — —, cubic control.

9. Embedding impedances

The impedance can also be evaluated using the power series expression, equation (6.1). Hence for optimized multipliers one obtains

$$Z_{in} = \frac{1}{\omega_p C_{min}} \left((k_1 - jk_2) \left(1 - \frac{C_{min}}{C_{max}} \right) - j \frac{C_{min}}{C_{max}} \right) + (k_3 - jk_4) R_s, \quad [\Omega], \qquad (9.1)$$

$$Z_n = \frac{1}{n\omega_p C_{min}} \left((k_1 + jk_2) \left(1 - \frac{C_{min}}{C_{max}} \right) + j \frac{C_{min}}{C_{max}} \right) + (k_3 + jk_4) R_s, \quad [\Omega] \qquad (9.2)$$

PHILOSOPHICAL TRANSACTIONS OF THE ROYAL SOCIETY A MATHEMATICAL, PHYSICAL & ENGINEERING SCIENCES

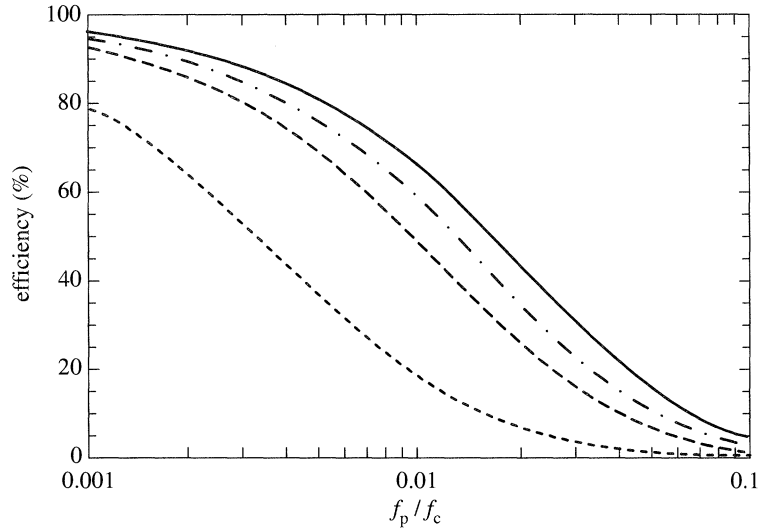

Figure 10. The maximum efficiency for a quintupler for different shapes of CV characteristic. All embedding impedances are adjusted for maximum efficiency, except for the lower curve where the idler is open circuited.

Table 1. *Coefficients for tripler impedance*

C–V model		k_1	k_2	k_3	k_4
flat	Z_{in}	0.030	0.101	0.84	0.21
flat	Z_3	0.22	0.18	0.66	−0.12
cubic	Z_{in}	0.046	0.21	0.78	0.25
cubic	Z_3	0.28	0.35	0.55	0.08
sharp	Z_{in}	0.063	0.33	0.71	0.31
sharp	Z_3	0.34	0.51	0.57	0.11

where Z_{in} is the diode impedance seen from the source and Z_n is the optimum embedding impedance load at the nth harmonic. Notice that if the series resistance R_s is much smaller than $1/(n\omega_\pi C_{min})$ the last term in these expressions can be neglected.

In a practical multiplier, it is difficult to achieve broadband performance if the reactive part of the impedance is large compared to the resistive part. Moreover, the losses in the coupling circuit are generally larger if the mismatch is large. A detailed investigation of the difference between the different cases, shows that 'Sharp $C(V)$', the most nonlinear case, offers a considerably more favourable ratio between the resistive part and the reactive part, particularly for the pump (input) frequency.

10. Experimental diodes

(*a*) *The first* GaAs *devices*

In the first experiments performed by (Rydberg *et al.* 1990), a GaAs–$Al_{0.7}Ga_{0.3}As$–GaAs diode was used, with a barrier width of 200 Å and on each side an undoped

Table 2. *Coefficients for quintupler impedance.*

C–V model		k_1	k_2	k_3	k_4
flat	Z_{in}	0.031	0.089	0.89	0.19
flat	Z_3	0	0.23	0	0.53
flat	Z_5	0.20	0.12	0.72	0.15
cubic	Z_{in}	0.057	0.19	0.88	0.27
cubic	Z_3	0	0.35	0	0.29
cubic	Z_5	0.26	0.24	0.62	0.22
sharp	Z_{in}	0.084	0.29	0.89	0.28
sharp	Z_3	0	0.48	0	0.30
sharp	Z_5	0.32	0.36	0.58	0.32

GaAs spacer of 50 Å. In the $Al_xGa_{1-x}As$–GaAs system, $Al_xGa_{1-x}As$ is an indirect bandgap semiconductor for aluminium concentrations $x > 0.41$. For $x = 0.7$, the $\Gamma \rightarrow \Gamma$ barrier energy is approximately 0.56 eV, and the $\Gamma \rightarrow X$ barrier energy is only 0.256 eV (Batey & Wright 1986). For a 200 Å barrier thickness, the $\Gamma \rightarrow X$ process should dominate. In fact, the measured barrier height of this varactor was determined to only 180 meV, which resulted in an unnecessarily large conduction current.

(*b*) *Improved* GaAs *barrier height*

By changing the barrier composition a much lower conduction current may be obtained. According to Krishnamurthi *et al.* (1994*b*), a barrier built from $Al_{0.4}Ga_{0.6}As$ with about 50 Å undoped GaAs spacers has a measured effective barrier height of 249 meV. Further improvement was achieved for a barrier composed from 62 Å $Al_{0.4}Ga_{0.6}As$ + 18 Å AlAs + 62 Å $Al_{0.4}Ga_{0.6}As$ surrounded by 50 Å $In_{0.2}Ga_{0.8}As$ spacers yielding an effective barrier height of 372 Å. Still the depletion regions are in GaAs.

(*c*) *Improved* $C_{\max}/C_{\min}$ *by doping the barrier*

By doping the barrier with n-type dopants 1.2×10^{17}, an improvement of the $C_{\max}$ to $C_{\min}$ ratio is obtained. However, this improvement will be at the expense of a larger leakage current. When this diode is compared in a multiplier with the one discussed below in § 10 *b*, there is no significant difference in multiplier performance.

(*d*) *One-barrier* InGaAs *devices*

At Lincoln Laboratory the first InGaAs diode was fabricated on an InP substrate (see table 3). Much less leakage current was obtained (Räisänen *et al.* 1995).

(*e*) *Three-barrier* InGaAs *devices*

Krishnamurthi *et al.* (1994*a*) suggested further improved varactors using $In_{0.53}Ga_{0.47}As$ for the depletion regions and three AlAs barriers (see table 4). To get a good ohmic contact at the top of the mesa structure a top layer of 1.5 μm heavily doped InGaAs was used. The lattice-matched epilayers were deposited on an n^{++} InP substrate by Philips Microwave, U.K. This particular epilayer combination yielded

Table 3. *Epitaxial layer structure of the Lincoln diode*

n^{++} InP substrate		
500 nm	InGaAs:Si	5×10^{18} cm^{-3}
250 nm	InGaAs	4×10^{17} cm^{-3}
25 nm	InGaAs	
25 nm	InAlAs	
25 nm	InGaAs	
250 nm	InGaAs:Si	4×10^{17} cm^{-3}
250 nm	InGaAs:Si	5×10^{18} cm^{-3}

Table 4. *Layer structure of device described in* § 7 *e*

n^{++} InP substrate			
1500 nm	$In_{0.53}Ga_{0.47}As$	1×10^{19} cm^{-3}	
250 nm	$In_{0.53}Ga_{0.47}As$	5×10^{16} cm^{-3}	
5 nm	$In_{0.53}Ga_{0.47}As$		
5 nm	$In_{0.52}Ga_{0.48}As$		
5 nm	AlAs		
5 nm	$In_{0.52}Ga_{0.48}As$		
5 nm	$In_{0.53}Ga_{0.47}As$		
350 nm	$In_{0.53}Ga_{0.47}As$	5×10^{16} cm^{-3}	} ×2
5 nm	$In_{0.53}Ga_{0.47}As$		
5 nm	$In_{0.52}Ga_{0.48}As$		
5 nm	AlAs		
5 nm	$In_{0.52}Ga_{0.48}As$		
5 nm	$In_{0.53}Ga_{0.47}As$		
250 nm	$In_{0.53}Ga_{0.47}As$	5×10^{16} cm^{-3}	
1500 nm	$In_{0.53}Ga_{0.47}As$	1×10^{19} cm^{-3}	

lower series resistance and higher power output capability for a given capacitance. The cut-off frequency for a 40 μm diameter device was 1.43 THz suggesting about 60% efficiency for a three times 14.3 GHz multiplier. A considerable advantage of this device is the high breakdown voltage of about 14 V.

(*f*) *Ten-barrier* InGaAs *devices*

A similar diode to the one of table 3 but with 10 barriers has been built by Philips Microwave on an InP substrate (Rahal *et al.* 1995). The conduction band discontinuity is as high as 0.53 eV. This structure was chosen as a compromise between low leakage and low capacitance per unit area. The C_{max}/C_{min} ratio was found to be 2.85. The calculated cut-off frequency of this device is as high as 1.5 THz. The breakdown voltage of this device was more than 20 V.

Table 5. *Suggested InAs diode structure*

n^{++} InAs substrate			
1000 nm	InAs:Si	4×10^{18} cm^{-3}	
200 nm	InAs:Si	5×10^{16} cm^{-3}	
7.5 nm	InAs		×3
14 nm	AlSb		
7.5 nm	InAs		
200 nm	InAs:Si	5×10^{16} cm^{-3}	
1000 nm	InAs:Si	4×10^{18} cm^{-3}	

(*g*) InAs *devices*

It will be very interesting if high quality diodes can be realized with InAs in the depletion region and in the top layer for ohmic contacts. The peak velocity in InAs is as high as 3.6×10^7 cm s^{-1}, i.e. more than 60% higher than in GaAs. The difference in mobility is even more dramatic. For undoped GaAs it is about 8000 cm^2 V^{-1} s^{-1} while for undoped InAs it is as high as 33 000 cm^2 V^{-1} s^{-1}. Moreover, the ohmic contact on InAs should be superior as well. Initial experiments on one- and two-barrier materials indicate difficulties in the fabrication of the material. Barriers containing AlAs have been shown to be very good for preventing conduction current, but contains a lot of traps affecting the *CV* characteristic at lower frequencies.

A suggested three-barrier structure is shown in table 5. Assuming the mobility in the doped layers is 10 000 cm^2 V^{-1} s^{-1}, the diode area 900 μm^2 and the ohmic contact is resistance per unit area is 5×10^7 cm^2 a cut-off frequency of 6.6 THz is calculated. For a three times 14 GHz this suggests an efficiency of about 90%. If R_s is 10 times higher, the efficiency drops to about 60%.

(*h*) *Characterization technique*

The capacitance versus voltage characteristic can be determined accurately from impedance measurements (Stake & Grönqvist 1995). It is difficult to measure the series resistance R_s, since it is rather small. The contribution in the series resistance comes mainly from the ohmic contact and the mesa, so it is possible to estimate R_s using a contact resistance measurement and resistivity data of the mesa material.

(*i*) *Experimental multipliers*

Despite a rather large current density obtained in this first diode, the conversion efficiency was reasonably high (Rydberg *et al.* 1990). The experiments were conducted in a Schottky-varactor waveguide tripler structure of the same design as described by Erickson (1982). For a range of 210–280 GHz a maximum efficiency of (see figure 9) about 5% and an output power of more than 1 mW was measured. This result was confirmed by Choudhury *et al.* (1993). For a good Schottky-varactor diode tripler for the same frequency range, using diodes from the University of Virginia (type 6P2), a maximum efficiency of about 5.5% was obtained (Rydberg *et al.* 1990). A theoretical analysis of the efficiency of diodes used yielded $\eta \approx 6.4\%$ in excellent agreement with the experimentally observed value of 5%.

A more ideal diode with the expected smaller conduction current should offer

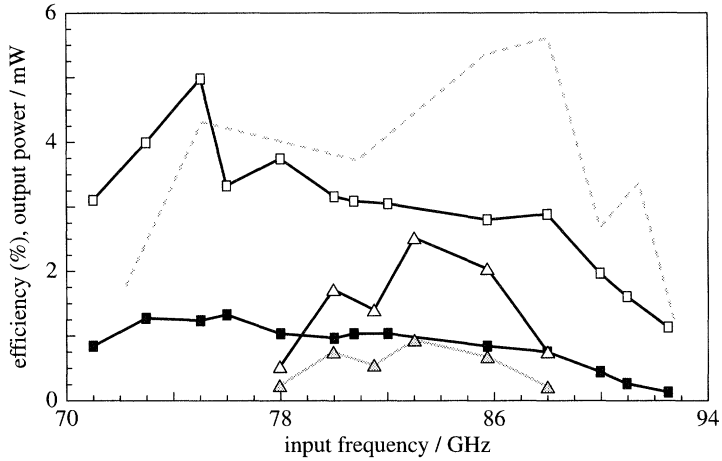

Figure 11. Measured efficiency and output power versus input frequency and theoretical output power for a SBV-tripler. The efficiency for a state-of-the-art Schottky-varactor diode using the same mount and idler configuration is also shown. (△) Efficiency for a 5×5 μm^2 (▲): output power for a 5×5 μm^2. (□): efficiency for a $\varnothing = 3$ μm diameter. (■): output power for a $\varnothing = 3$ μm. (- · - · -): theoretical output power for 24 mW input power. (- - -): efficiency for a Schottky-varactor diode (type: 6P2).

$\eta \approx 13.6\%$ efficiency for 32 mW input power. An ohmic contact resistance for the mesas of $3 \times 10^{-6}\ \Omega\ cm^2$ and a total series resistance of *ca.* 25 Ω was assumed in the analysis (Rydberg & Grönqvist 1989).

Krishnamurthi *et al.* (1995) have investigated a planar multiplier using the three-barrier stacked diode described in table 4. The multiplier was a tripler for 3×13.45 GHz. The measured output power was 6.2 dB less than predicted for the ideal case, but can be partly explained by a non-ideal output circuit (Krishnamurthi 1995). The same diode was also tried by Philips Microwave (Rogers 1993) in a waveguide mount yielding an output power of 20 dBm and a conversion efficiency of 20%. The second harmonic was found to be well rejected with a value of −38 dB with respect to the third harmonic.

Rahal *et al.* (1995) have investigated a 3×31 GHz multiplier using the ten-barrier InGaAs diode described above and a waveguide mount. An output power of 20 dBm for a flange-to-flange conversion loss of 20% was obtained. This efficiency can be compared with a predicted maximum conversion of about 60% (using figure 8).

Räisänen *et al.* (1995) have carried out experiments on quintuplers 5×35 using the GaAs diode (*c*) as well as the Lincoln Lab InGaAs diode described above (*d*). They used a crossed waveguide mount quintupler structure in which the input and output waveguides were separated by a low-pass filter. The efficiency obtained was 0.93% for 14 mW input power with the InGaAs diode (*d*) and 0.65% for 22 mW input power for the GaAs diode (*c*).

11. Conclusions

We have pointed out the advantages of HBV for generating millimetre waves. The varactor has in the authors opinion the largest potential for high power generation at millimetre-wave frequencies. In particular, it is possible to utilize advanced bandgap engineering including pure InAs materials. Such materials are predicted to give the highest efficiency due to the low parasitic resistances in the diode.

References

Batey, J. & Wright, S. L. 1986 Energy band alignment in GaAs: (Al,Ga)As heterojunctions: the dependence on alloy composition. *J. Appl. Phys.* **59**, 200–209.

Choudhury, D., Frerking, M. A. & Batelaan, P. D. 1993 A 200-GHz tripler using a single barrier varactor. *IEEE Trans. Microwave Theory Technol.* **41**, 595–599.

Dillner, L., Stake, J. & Kollberg, E. L. 1995 Analysis of symmetric frequency varactor multipliers. Report no. 27, Department of Microwave Technology, Chalmers University of Technology, Göteborg, Sweden, ISSN 1103-4599, ISRN CTH-MVT-R–27–SE.

Erickson, N. R. 1982 A high efficiency frequency tripler for 230 GHz. *12th European Microwave Conf.*

Grönqvist, H., Kollberg, E. L. & Rydberg, A. 1991 Quantum-well and quantum-barrier diodes for generating submillimeter wave power. *Microwave Opt. Technol. Lett.* **4**, 33–38.

Jones, J. R., Jones, S. H., Tait, G. B. & Zybura, M. F. 1994 Heterostructure barrier varactor simulation using an integrated hydrodynamic device/harmonic-balance circuit analysis technique. *IEEE Microwave Guided Wave Lett.* **4**, 411–413.

Jones, J. R., Tait, G. B., Jones, S. H. & Katzer, S. D. 1995 DC and large-signal time-dependent electron transport in heterostructure devices: an investigation of the heterostructure barrier varactor. *IEEE Trans. Electron Dev.* **42**, 1393–1403.

Kollberg, E. L. & Rydberg, A. 1989 Quantum-barrier-varactor diode for high efficiency millimeter-wave multipliers. *Electron. Lett.* **25**, 1696–1697.

Kollberg, E. L., Tolmunen, T. J., Frerking, M. A .& East, J. R. 1992 Current saturation in submillimeter wave varactors. *IEEE Trans. Microwave Theory Technol.* **40**, 831–838.

Krishnamurthi, K. 1995 Heterostructure varactors on InP and GaAs for millimeter-wave frequency triplers. Ph.D. Thesis, Department of Electronics, Carleton University, Ottawa.

Krishnamurthi, K., Boch, E. & Harrison, R. G. 1995 A Ka-band planar tripler based on a stacked symmetric InP heterostructure-barrier varactor. *IEEE–MTT Int. Microwave Symp. Digest* (Orlando, FL).

Krishnamurthi, K. & Harrison, R. G. 1993 Analysis of symmetric-varactor frequency triplers. *IEEE–MTT Int. Microwave Symp. Digest.*

Krishnamurthi, K., Harrison, R. G., Rogers, C., Ovey, J., Nilsen, S. M. & Missous, M. 1994*a* Stacked heterostructure barrier varactors on InP for millimeter wave triplers. *Fifth Int. Symp. on Space Terahertz Technology.*

Krishnamurthi, K., Nilsen, S. M. & Harrison, R. G. 1994*b* GaAs Single-barrier varactors for millimeter-wave triplers: guidelines for enhanced performance. *IEEE Trans. Microwave Theory Technol.* **42**, 2512–2516.

Lieneweg, U., Hancoock, B. R. & Maserjian, J. 1987 Barrier-intrinsic-N+ (BIN) diodes for near-millimeter wave generation. *Int. Conf. Infrared and Millimeter-Waves.*

Nilsen, S. M., Grönqvist, H., Hjelmgren, H., Rydberg, A. & Kollberg, E. L. 1993 Single barrier varactors submillimeter wave power generation. *IEEE Trans. Microwave Theory Technol.* **41**, 572–580.

Peatman, W. C. B., Crowe, T. W. & Shur, M. 1992 A novel Schottky/2-DEG diode for millimeter- and submillimeter-wave multiplier applications. *IEEE Electron Dev. Lett.* **13**, 11–13.

Rahal, A.,. Bosisio, R. G, Rogers, C., Ovey, J. & Missous, M. 1995 A multi-stack quantum barrier varactor on InP for MM-wave frequency tripling (Bologna).

Rogers, C. 1993 Stacked quantum barrier high power multiplier varactors. Hazel Grove, UK, Philips Microwave.

Rydberg, A. & Grönqvist, H. 1989 Quantum-well high-efficiency millimetre-wave frequency tripler. *Electron. Lett.* **25**, 348–349.

Rydberg, A., Grönqvist, H. & Kollberg, E. L. 1990 Millimeter- and submillimeter-wave multipliers using quantum-barrier-varactor (QBV) diodes. *IEEE Trans. Electron Dev.* **11**, 373–375.

Rydberg, A., Grönqvist, H. & Kollberg, E. L. 1992 Reply to comments on millimeter- and submillimeter-wave multipliers using quantum-barrier-varactor (QBV) diodes. *IEEE Trans. Electron Dev.* **13**, 132–133.

PHILOSOPHICAL TRANSACTIONS OF THE ROYAL SOCIETY A MATHEMATICAL, PHYSICAL & ENGINEERING SCIENCES

Räisänen, A. V., Tolmunen, T. J., Natzic, M., Frerking, M. A., Brown, E., Grönqvist, H. & Nilsen, S. M. 1995 A single barrier varactor quintupler at 170 GHz. *IEEE Trans. Microwave Theory Technol.* **43**, 685–688.

Sollner, T. C. L. G., Brown, E. R., Goodhue, W. D. & Le, H. Q. 1987 Observations of millimeter-wave oscillations from resonant tunneling diodes and some theoretical considerations of ultimate frequency limits. *Appl. Phys. Lett.* **50**, 332–334.

Stake, J. & Grönqvist, H. 1995 An on-wafer method for C–V characterisation of heterostructure diodes. *Microwave Opt. Technol. Lett.* **9**, 63–66.

Sze, S. M. 1981 *Physics of semiconductor devices.* Singapore: Wiley.

Tang, C. C. H. 1966 An exact analysis of varactor frequency multiplier. *IEEE Trans. Microwave Theory Technol.* 210–212.

Tolmunen, T. J., Nilsen, S. M., Boric, O., Frerking, M. A. & Kollberg, E. L. 1991 Accurate characterisation of varactors with fF capacitance. *16th Int. Conf. Infrared and Millimeter Waves* (Lausanne).

Yngvesson, S. 1991 *Microwave semiconductor devices.* Amsterdam: Kluwer.

PHILOSOPHICAL TRANSACTIONS OF THE ROYAL SOCIETY A MATHEMATICAL, PHYSICAL & ENGINEERING SCIENCES